CPC(HEP & NP), 2011, **35**(8): 741–746 Chinese Physics C Vol. 35, No. 8, Aug., 2011

Hypertriton and light nuclei production at Λ-production subthreshold energy in heavy-ion collisions*

ZHANG Song(张松)[1] CHEN Jin-Hui(陈金辉)[1;1)] MA Yu-Gang(马余刚)[1;2)] XU Zhang-Bu(许长补)[2]
CAI Xiang-Zhou(蔡翔舟)[1] MA Guo-Liang(马国亮)[1] ZHONG Chen(钟晨)[1]

[1] Shanghai Institute of Applied Physics, the Chinese Academy of Sciences, Shanghai 201800, China
[2] Brookhaven National Laboratory, Upton, New York, 11973, USA

Abstract: High-energy heavy-ion collisions produce abundant hyperons and nucleons. A dynamical coalescence model coupled with the ART model is employed to study the production probabilities of light clusters, deuteron (d), triton (t), helion (^{3}He), and hypertriton ($^3_\Lambda$H) at subthreshold energy of Λ production (≈1 GeV per nucleon). We study the dependence on the reaction system size of the coalescence penalty factor per additional nucleon and entropy per nucleon. The Strangeness Population Factor $\left(S_3={}^3_\Lambda\mathrm{H}/\left({}^3\mathrm{He}\times\frac{\Lambda}{\mathrm{p}}\right)\right)$ shows an extra suppression of hypertriton comparing to light clusters of the same mass number. This model predicts a hypertriton production cross-section of a few μb in ^{36}Ar+^{36}Ar, ^{40}Ca+^{40}Ca and ^{56}Ni+^{56}Ni in 1 *A* GeV reactions. The production rate is as high as a few hypertritons per million collisions, which shows that the fixed-target heavy-ion collisions at CSR (Lanzhou/China) at Λ subthreshold energy are suitable for breaking new ground in hypernuclear physics.

Key words: hyperon, hypernuclei, dynamic coalescence

PACS: 25.75.Gz, 12.38.Mh, 24.85.+p **DOI:** 10.1088/1674-1137/35/8/008

1 Introduction

In a laboratory environment, heavy-ion collisions are the main way to study the behavior of nuclear matter and hadron interactions as well as to investigate QCD matter under conditions of extreme energy and baryon density [1]. In addition, abundant hadrons containing strange valence quarks can be produced in these collisions, which provides the opportunity to observe multi-strange bound systems. Hypernuclei, nuclei containing at least one hyperon, provide a doorway to the production of strangelets [2], and a unique opportunity to study the hyperon-nucleon (Y-N) and hyperon-hyperon (Y-Y) interactions [3]. The measurements of Y-N and Y-Y interactions are essential for the theoretical study of neutron stars [4] and exotic states of finite nuclei [5].

The formation of hypernuclei is determined by probabilities of the overlapping of the wave functions of nucleons and Λ hyperons at the final stage of the collisions [6, 7]. Consequently, hypernucleus yields provide information about the local density correlation of baryons and strangeness on an event-by-event basis [8] as triton (t) and helium (^{3}He) are a measurement of baryon correlation [9]. In addition, the Strangeness Population Factor (S_3) characterizes the local density correlation strength between baryon number and strangeness [10]. Measurements at RHIC and AGS energies show that there is an extra suppression factor in the coalescence production of $^3_\Lambda$H compared with ^{3}He [11] at AGS, while the same measurement of S_3 is close to unity at RHIC [12].

Light nuclei, produced by the coalescence of nucleons, show a striking exponential dependence on nuclear mass number with a penalty factor [2]. Projections based on these measurements can be used to

Received 15 November 2010
* Supported by National Natural Science Foundation of China (Y155017011, 10775167, 10875159, 10905085, 11035009, 11047116), and Knowledge Innovation Project of Chinese Academy of Sciences (KJCX2-EW-N01)
1) E-mail: chenjinhui@sinap.ac.cn
2) E-mail: ygma@sinap.ac.cn

estimate the production probabilities of strangelets [2] and hypernuclei [11, 13]. The ratio of $N_\mathrm{d}/N_\mathrm{p}$ will be proportional to the entropy per nucleon in the fireball [13, 14]. Alternatively, the yields can be explained in a thermal model without invoking dynamic models [15].

Recently, the STAR collaboration at RHIC (Brookhaven) reported the observation of antihypertritons in Au + Au collisions at $\sqrt{s_\mathrm{NN}}$=200 GeV [12]. Future experiments with a high energy heavy-ion beam are proposed to further investigate nuclear matter and hadron physics as well as search for phase transition to quark-gluon plasma at high baryon density. Hypernucleus measurements and potential discoveries of new exotic hypernuclei at these new facilities can provide important information about Y-N and Y-Y interactions [16]. Specifically, the hypertriton lifetime and binding energy are very sensitive to Y-N interactions [17]. However, measurements over the last few decades have been inconclusive because of insufficient statistics [12, 18].

In this paper, a dynamical coalescence model [19] coupled with a transport model is developed to study the production rates of ${}^3_\Lambda$H and light nuclei, i.e. d, t and ^{3}He. The calculations are with ^{12}C, ^{24}Mg, ^{36}Ar, ^{40}Ca and ^{56}Ni beams of energy at 1 A GeV on equal-mass targets. We study the rapidity distributions of p, Λ, d, t, ^{3}He and ${}^3_\Lambda$H, extracting the penalty factor for light clusters, the S_3 based on ${}^3_\Lambda$H and the entropy per nucleon. Based on these results, we discuss the production probabilities of hypernuclei and light nuclei as well as local hyperon-baryon correlations. We note that similar calculations based on the transport equation of the Boltzmann type [20], or the canonical thermodynamic model [21] at GSI, FAIR or J-PARC energy have been carried out recently. We here focus on the Λ subthreshold energy for fixed-target heavy-ion collisions at CSR (Lanzhou/China) [22].

2 A dynamical coalescence model

The dynamic coalescence model has been a popular approach for describing the production of light clusters in heavy-ion collisions [19], and has been used at both intermediate [23] and high energies [10, 24]. The clusters are formed on the basis of the hadron phase-space distribution at freeze-out in the model. The probability of producing a cluster is determined by its Wigner phase-space density without taking the binding energies into account [23, 24]. The multiplicity of a M-hadron cluster in heavy-ion collisions is given by [23, 24],

$$N_\mathrm{M} = G\int \mathrm{d}\boldsymbol{r}_{i_1}\mathrm{d}\boldsymbol{q}_{i_1}\cdots\mathrm{d}\boldsymbol{r}_{i_{M-1}}\mathrm{d}\boldsymbol{q}_{i_{M-1}} \times\left\langle \sum_{i_1>i_2>\cdots>i_M}\rho_i^\mathrm{W}(\boldsymbol{r}_{i_1},\boldsymbol{q}_{i_1}\cdots\boldsymbol{r}_{i_{M-1}},\boldsymbol{q}_{i_{M-1}})\right\rangle. \tag{1}$$

In Eq. (1), $\boldsymbol{r}_{i_1}$, $\cdots$, $\boldsymbol{r}_{i_{M-1}}$ and $\boldsymbol{q}_{i_1}$, $\cdots$, $\boldsymbol{q}_{i_{M-1}}$ are, respectively, the $M-1$ relative coordinates and momenta in the M-hadron rest frame; ρ_i^W is the Wigner phase-space density of the M-hadron cluster, and $\langle\cdots\rangle$ denotes the event averaging. G represents the statistical factor for the cluster; it is 3/8 for d, 1/3 for t, ^{3}He [23–25] and ${}^3_\Lambda$H (Λ and ${}^3_\Lambda$H have the same spin as the neutron and triton, respectively).

To determine the Wigner phase-space densities, we take their hadron wave functions to be those of a spherical harmonic oscillator [23, 26]. For the deuteron, its hadron wave function is

$$\psi(\boldsymbol{r}_1,\boldsymbol{r}_2)=1/(\pi\sigma_\mathrm{d}^2)^{3/4}\exp[-r^2/(2\sigma_\mathrm{d}^2)], \tag{2}$$

in terms of the relative coordinate $\boldsymbol{r}=\boldsymbol{r}_1-\boldsymbol{r}_2$ and the size parameter σ_d. The root mean square radius can be deduced as $R_\mathrm{d}=\langle r^2\rangle^{1/2}=(3/8)^{1/2}\sigma_\mathrm{d}$ for deuteron.

The hadron Wigner phase space density function inside the deuteron can be obtained from its hadron wave function by

$$\begin{aligned}\rho_\mathrm{d}^\mathrm{W}(\boldsymbol{r},\boldsymbol{k}) &= \int\psi\left(\boldsymbol{r}+\frac{\boldsymbol{R}}{2}\right)\psi^*\left(\boldsymbol{r}-\frac{\boldsymbol{R}}{2}\right) \times\exp\left(-\mathrm{i}\boldsymbol{k}\cdot\boldsymbol{R}\right)\mathrm{d}^3\boldsymbol{R}\\ &= 8\exp\left(-\frac{r^2}{\sigma_\mathrm{d}^2}-\sigma_\mathrm{d}^2k^2\right),\end{aligned} \tag{3}$$

where $\boldsymbol{k}=(\boldsymbol{k}_1-\boldsymbol{k}_2)/2$ is the relative momentum between hadrons inside the deuteron.

For t, ^{3}He and ${}^3_\Lambda$H, the hadron wave function is the same and is given by that of a spherical harmonic oscillator [23, 26],

$$\psi=(3/\pi^2b^4)^{-3/4}\exp\left(-\frac{\rho^2+\lambda^2}{2b^2}\right), \tag{4}$$

the Wigner phase-space density is then given by

$$\rho_3^\mathrm{W}=8^2\exp\left(-\frac{\rho^2+\lambda^2}{b^2}\right)\exp\left(-(\boldsymbol{k}_\rho^2+\boldsymbol{k}_\lambda^2)b^2\right). \tag{5}$$

In Eq. (4) and (5), normal Jacobian coordinates for a three-particle system are introduced in Ref. [23]. (ρ, λ) and ($\boldsymbol{k}_\rho$, $\boldsymbol{k}_\lambda$) are, respectively, the relative coordinates and momenta. The root mean square radius R_3 of a 3-hadron cluster is given by

$$R_3=\left[\int\frac{\rho^2+\lambda^2}{3}|\psi(\boldsymbol{r}_1,\boldsymbol{r}_2,\boldsymbol{r}_3)|^2 3^{3/2}\mathrm{d}\rho\mathrm{d}\lambda\right]^{1/2}=b. \tag{6}$$

The root mean square radii are 1.92, 1.61, 1.74 and 5 fm for d, t, ^{3}He and $^3_\Lambda$H [11, 23], respectively. The time-space and energy-momentum distribution of hadrons (proton, neutron and Λ) at freeze-out are from ART1.0 [27]. The overlapping Wigner phase space density can be calculated by Eq. (3) for a 2-hadron cluster and Eq. (5) for a 3-hadron cluster and the multiplicity of these clusters is determined by Eq. (1). It is apparent that this coalescence mechanism results in correlations between the momenta and the positions of hadrons at freeze-out. The production of light (hyper) clusters is related to the multiplicity of hadrons (hyperons) and the size parameter of the root mean square radii of these objects.

3 Introduction to ART1.0 model

Based on the Boltzmann-Uhlenbeck (BUU) model [28] for intermediate energy heavy-ion collisions, ART1.0 is developed for heavy-ion collisions at AGS energies [27] by including more baryon and meson resonances and their interactions, such as baryons N, Δ(1232), N*(1440), N*(1535), Λ, Σ and mesons π, ρ, ω, η, K. The elastic and inelastic collision cross sections and angular distributions among most of these particles are from Ref. [29] in ART1.0 model. Most inelastic hadron-hadron collisions are simulated through the formation of resonances. Λ hyperon production is mainly associated with K$^-$ meson production through baryon-baryon collisions,

$$\begin{cases} \mathrm{NN} \rightarrow \mathrm{N}\Lambda(\Sigma)\mathrm{K},\ \Delta\Lambda(\Sigma)\mathrm{K}, \\ \mathrm{NR} \rightarrow \mathrm{N}\Lambda(\Sigma)\mathrm{K},\ \Delta\Lambda(\Sigma)\mathrm{K}, \\ \mathrm{RR} \rightarrow \mathrm{N}\Lambda(\Sigma)\mathrm{K},\ \Delta\Lambda(\Sigma)\mathrm{K}, \end{cases} \tag{7}$$

where R denotes a Δ, N*(1440), or N*(1535), and meson-baryon interactions,

$$\begin{cases} \pi+\mathrm{N}(\Delta,\mathrm{N}^*) \rightarrow \Lambda(\Sigma)+\mathrm{K}, \\ \rho+\mathrm{N}(\Delta,\mathrm{N}^*) \rightarrow \Lambda(\Sigma)+\mathrm{K}, \\ \omega+\mathrm{N}(\Delta,\mathrm{N}^*) \rightarrow \Lambda(\Sigma)+\mathrm{K}. \end{cases} \tag{8}$$

We first checked the rapidity distribution of Λ in ^{56}Ni + ^{56}Ni collisions at a beam energy of 1.93 A GeV from ART1.0 model with the same kinematic windows as for FOPI data analysis in 2007 [30], shown in Fig. 1.

The results from ART1.0 are consistent with the data [30, 31]. Λ are mainly produced at mid-rapidity and quickly decrease towards forward (backward) rapidity. We then calculated the rapidity distributions in ^{12}C+^{12}C, ^{24}Mg+^{24}Mg, ^{36}Ar+^{36}Ar, ^{40}Ca+^{40}Ca and ^{56}Ni+^{56}Ni reactions at beam energy of 1 A GeV, shown in the left and right panels of Fig. 2 for protons and Λ, respectively. The proton rapidity distributions are different from those for Λ: protons are mainly produced at forward and backward rapidity while Λs are at mid-rapidity. Since the ART model does not allow for the possibility that composite fragments ($A > 1$) exist in the final state of the collision, the production

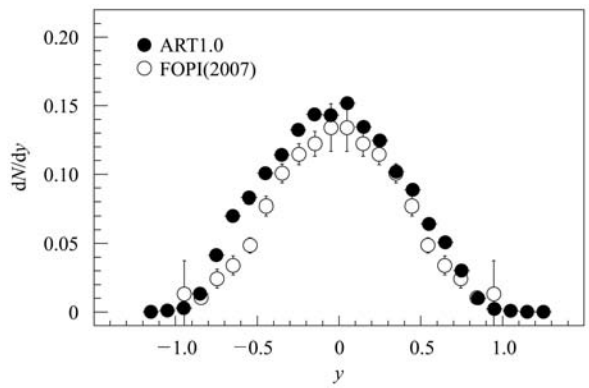

Fig. 1. Λ rapidity distribution in ^{56}Ni+^{56}Ni collisions at beam energy of 1.93 A GeV with impact parameter b<3.1 fm. solid circles: the ART1.0 model; open circles: the FOPI data [30].

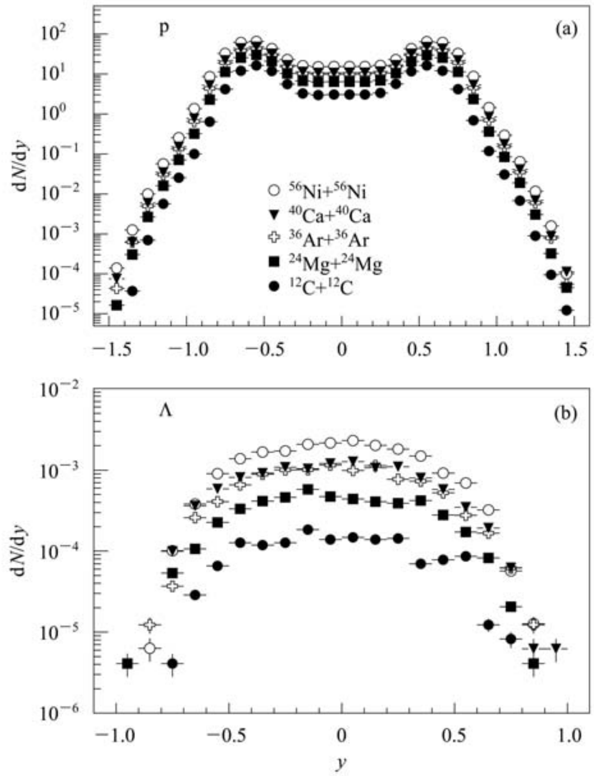

Fig. 2. The rapidity distribution of p (a) and Λ (b) in 0%–80% centrality ^{12}C+^{12}C, ^{24}Mg+^{24}Mg, ^{36}Ar+^{36}Ar, ^{40}Ca+^{40}Ca and ^{56}Ni+^{56}Ni reactions at beam energy of 1 A GeV from ART1.0 model.

of protons at forward and backward rapidity is enhanced (cf. Fig. 2). We here include a dynamical coalescence model (as detailed in Section 2) as an afterburner to calculate the light cluster production. The contribution of protons at forward and backward rapidity to light clusters at mid-rapidity is minor, based on Eqs. (1), (3) and (5). The contribution to hypertritons can be neglected when the rapidity distribution of Λ is taken into account.

4 Results

4.1 Rapidity distributions

Figure 3 shows the rapidity distributions of d, t, ^{3}He and $^3_\Lambda$H in ^{12}C+^{12}C, ^{24}Mg+^{24}Mg, ^{36}Ar+^{36}Ar, ^{40}Ca+^{40}Ca and ^{56}Ni+^{56}Ni reactions at 1 A GeV from ART1.0 model plus a dynamical coalescence model. As per Eqs. (1) and (3), we assume that the production probabilities of d, t and ^{3}He are proportional to the densities of protons and neutrons. In the case of $^3_\Lambda$H, the density of Λ is also a factor. As observed in Fig. 3, the light clusters are mainly at forward and backward rapidity, similar to the distribution of protons. The rapidity of $^3_\Lambda$H is determined by nucleons and Λs.

The inclusive yields of d, t, ^{3}He and $^3_\Lambda$H with nucleons and Λ in this calculation are listed in Table 1.

Our calculations yield the $^3_\Lambda$H production rate of 10^{-2} μb in ^{12}C+^{12}C at 1 A GeV reactions, 10^{-1} μb in ^{24}Mg+^{24}Mg at 1 A GeV, a few μb in ^{36}Ar+^{36}Ar, ^{40}Ca+^{40}Ca and ^{56}Ni+^{56}Ni at 1 A GeV reactions. The total reaction cross section for ^{12}C+^{12}C collisions is $\sim 10^3$ mb at beam energy of ~ 1 A GeV [32]. We here take 10^3 mb in the total yield calculation from ^{12}C to ^{56}Ni system. Our results are close to the recent transport model calculation [20], where light hypernuclei production probabilities are a few μb in ^{12}C+^{12}C at 2 A GeV reactions.

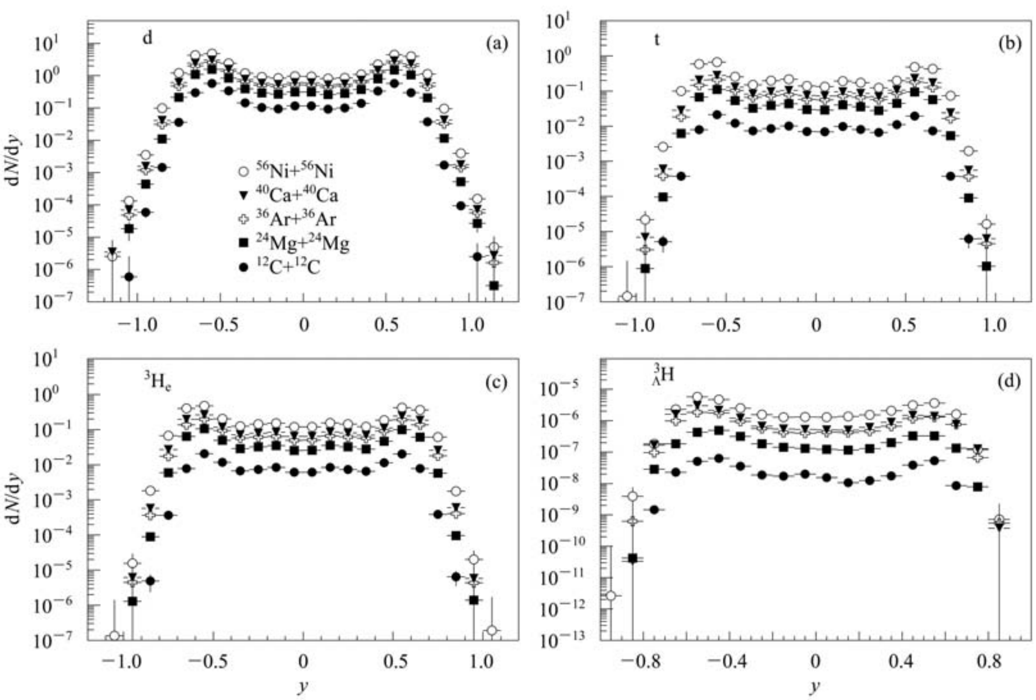

Fig. 3. The rapidity distributions of d (a), t (b), ^{3}He (c) and $^3_\Lambda$H (d) in 0%–80% centrality ^{12}C+^{12}C, ^{24}Mg+^{24}Mg, ^{36}Ar+^{36}Ar, ^{40}Ca+^{40}Ca and ^{56}Ni+^{56}Ni reactions at a beam energy of 1 A GeV.

Table 1. The total yield per event of p, Λ, d, t, ^{3}He and $^3_\Lambda$H in 0%–80% centrality ^{12}C+^{12}C, ^{24}Mg+^{24}Mg, ^{36}Ar+^{36}Ar, ^{40}Ca+^{40}Ca and ^{56}Ni + ^{56}Ni at 1 A GeV reaction from ART1.0 model plus a dynamical coalescence model calculation. The rapidity range is $-1<y<1$.

	p	Λ	d	t	^{3}He	$^3_\Lambda$H
^{12}C + ^{12}C	11.985	1.480×10^{-4}	0.340	0.014	0.014	3.848×10^{-8}
^{24}Mg + ^{24}Mg	23.969	4.864×10^{-4}	0.980	0.072	0.068	3.268×10^{-7}
^{36}Ar + ^{36}Ar	35.955	1.010×10^{-3}	1.687	0.142	0.135	1.233×10^{-6}
^{40}Ca + ^{40}Ca	39.949	1.155×10^{-3}	1.990	0.186	0.177	1.618×10^{-6}
^{56}Ni + ^{56}Ni	55.916	2.006×10^{-3}	3.225	0.411	0.326	3.441×10^{-6}

4.2 Dependence of light cluster production on nuclear mass number

In the following, we investigate the nuclear mass number dependence of light cluster production, shown in Fig. 4.

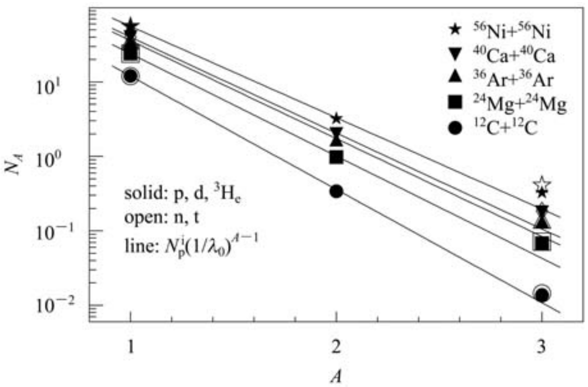

Fig. 4. The yields of light clusters as a function of nuclear mass number from 0%–80% centrality at 1 A GeV nuclei reaction.

The fit function is [33]

$$N_A = N_{\mathrm{p}}^i \left(\frac{1}{\lambda_0}\right)^{A-1}. \tag{9}$$

where N_{p}^i, λ_0 and A denote the total mass number of initial protons, the penalty factor and the nuclear mass number, respectively. The penalty factor quantitatively represents how hard it is to produce the next massive cluster (A+1) compared with the current cluster (A). Therefore, it can be applied to estimate the production rates of heavy clusters. For example, the yields of light clusters show an exponential dependence on the nuclear mass number with a penalty factor of ∼34 per additional nucleon for ^{12}C+^{12}C reactions and ∼17 for ^{56}Ni+^{56}Ni reactions. The penalty factors for different reaction systems, shown in Fig. 5, decrease with increasing size of the reaction system from ^{12}C+^{12}C to ^{56}Ni+^{56}Ni reactions.

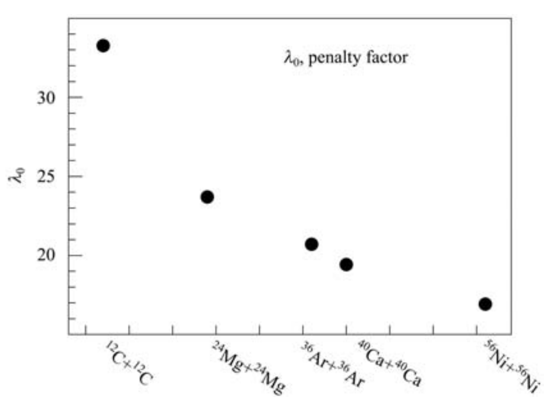

Fig. 5. The penalty factor as a function of reaction system at 0%–80% centrality 1 A GeV reaction.

This decreasing trend implies that the production probabilities of current analyzed light clusters are higher in colliding system with a larger total mass number. It is argued that if strangelets are created in the reactions, an extra suppression factor with total strangeness in this 'cluster' should be added in the fit function [33]. However, there has been no positive observation of strangelets so far [2].

The penalty factor also reflects the entropy per nucleon [13, 14], defined as

$$S_{\mathrm{N}} = 3.945 - \ln\left(\frac{N_{\mathrm{d}}}{N_{\mathrm{p}}}\right). \tag{10}$$

Considering Eq. (9), one knows that the ratio of $N_{\mathrm{d}}/N_{\mathrm{p}}$ is inversely proportional to the penalty factor, λ_0. Then Eq. (10) can be rewritten as

$$S_{\mathrm{N}} = 3.945 - \ln\left(\frac{1}{\lambda_0}\right). \tag{11}$$

The calculations from Eqs. (10) and (11) are presented in Fig. 6 and are consistent with each other.

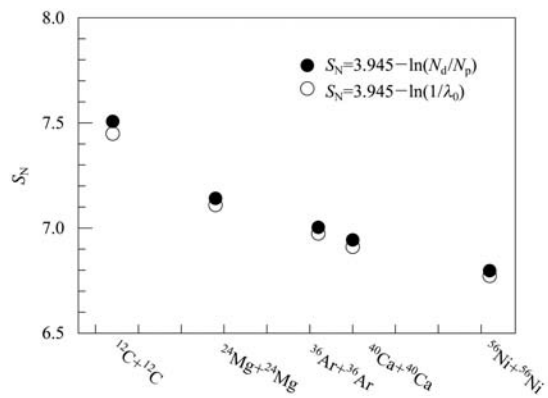

Fig. 6. The entropy per nucleon as a function of reaction system from 0%–80% centrality 1 A GeV reaction.

A widespread interpretation in intermediate-energy heavy-ion collisions is that deuterons can form before chemical freeze-out and can break up and reform a number of times before freeze-out [13, 14]. During this stage of the reaction, the deuteron density reaches an equilibrium. In fact, the ratio of $N_{\mathrm{d}}/N_{\mathrm{p}}$ just depends on the mean density of nucleons in phase space [14]. Consequently, the ratio $N_{\mathrm{d}}/N_{\mathrm{p}}$ is proportional to the entropy per nucleon, S_{N} [13, 14]. Our S_{N} calculation is consistent with that in Ref. [13] ($S_{\mathrm{N}} = 7.0$) and with the value obtained by E814 [34] ($S_{\mathrm{N}} = 12.8$). Values of $N_{\mathrm{d}}/N_{\mathrm{p}}$ from a thermal model [15] result in S_{N} predictions around 6 at AGS energies, 7 to 8 at SPS, and 10 at RHIC. This beam energy dependence reflects the decreasing probability of forming composite fragments as the beam energy increases.

4.3 Strangeness Population Factor

Since S_3

$$S_3 = {}^{3}_{\Lambda}\text{H}/\left({}^{3}\text{He}\times\frac{\Lambda}{\text{p}}\right)$$

is a good representation of the local correlation between baryon number and strangeness [10], a comprehensive analysis including the previous work focus on RHIC energy [10] will shed light on the nature of the nuclear matter created in heavy-ion reactions. Fig. 7 shows the results in our model at CSR energy: the S_3 is ~ 0.23 in ^{12}C+^{12}C and ^{24}Mg+^{24}Mg reactions and $\sim$0.3 in ^{36}Ar + ^{36}Ar, ^{40}Ca+^{40}Ca and ^{56}Ni+^{56}Ni reactions.

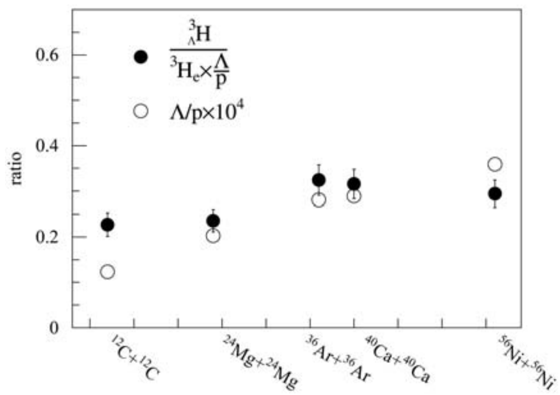

Fig. 7. The Strangeness Population Factor as a function of reaction system. The Λ to proton ratio with a scale factor 10^4 is also plotted for reference.

The ${}^{3}_{\Lambda}$H is further suppressed with respect to the ^{3}He when including strangeness into particle production at Λ subthreshold energy. These new calculations are in agreement with the value obtained by E864 (S_3=0.36) at AGS energy [11], and are consistent with a dramatic increase in the baryon-strangeness correlation from beam energies at Λ subthreshold energy and AGS to RHIC [12].

5 Summary

In summary, we calculate the production rate for light clusters, including hypertritons, in heavy-ion reactions at Λ subthreshold energy with the ART1.0 model plus a dynamical coalescence model as an afterburner. We find that the production rate of hypertriton reaches a few μb in ^{36}Ar+^{36}Ar, ^{40}Ca+^{40}Ca and ^{56}Ni+^{56}Ni at 1 A GeV reactions. Our calculation shows that the fixed-target (from ^{36}Ar to ^{56}Ni) heavy-ion collisions at CSR (Lanzhou/China) are suitable for hypernucleus production. A sample of a few hundred hypertritons is expected to be detected with a three-week dedicated run.

References

1 Arsene I et al. Nucl. Phys. A, 2005, **757**: 1; Back B B et al. Nucl. Phys. A, 2005, **757**: 28; Adams J et al. Nucl. Phys. A, 2005, **757**: 102; Adler S S et al. Nucl. Phys. A, 2005,**757**: 184
2 Barrette J et al. Phys. Lett. B, 1990, **252**: 550
3 Wroblewski A D. Acta Phys. Pol. B, 2004, **35**: 901
4 Schaffner J, Mishustin I. Phys. Rev. C, 1996, **53**: 1416
5 Hofmann F, Keil C M, Lenske H. Phys. Rev. C, 2001, **64**: 025804
6 Danysz M, Pniewski J. Phil. Mag., 1953, **44**: 348
7 Kerman A K, Weiss M S. Phys. Rev. C, 1973, **8**: 408; Gutbrod H H et al. Phys. Rev. Lett., 1976, **37**: 667
8 Steinheimer J et al. Phys. Lett. B, 2009, **676**: 126
9 Sato H, Yazaki K. Phys. Lett. B, 1981, **98**: 153
10 Zhang S et al. Phys. Lett. B, 2010, **684**: 224
11 Armstrong T A et al. Phys. Rev. C, 2004, **70**: 024902
12 Abelev B I et al. Science, 2010, **328**: 58
13 Albergo S et al. Phys. Rev. C, 2002, **65**: 034907
14 Siemens P J and Kapusta J I. Phys. Rev. Lett., 1979, **43**: 1486
15 Andronic A, Braun-Munzinger P, Stachel J. Phys. Lett. B, 2009, **673**: 142
16 Beane S R, Bedaque P F, Parreno A, Savage M J. Nucl. Phys. A, 2005, **747**: 55; Beane S R et al. Nucl. Phys. A, 2007, **794**: 62
17 Dalitz R H, Rajasekharan G. Phys. Lett., 1962, **1**: 58; Kamada H, Golak J, Miyagawa K, Witala H, Glöckle W. Phys. Rev. C, 1998, **57**: 1595
18 Davis D H. Nucl. Phys. A, 1992, **547**: 369
19 Csernai L P, Kapusta J I. Phys. Rep., 1986, **131**: 223
20 Gaitanos T, Lenske H, Mosel U. Phys. Lett. B, 2009, **675**: 297
21 Gupta S Das. Nucl. Phys. A, 2009, **822**: 41; Pop V Topor, Gupta S Das. Phys. Rev. C, 2010, **81**: 054911
22 Jing H T, Shen P N, Jiang H Q. HEP & NP, 2007, **31**: 10 (in Chinese); YANG X D et al. Chin. Phys. C (HEP & NP), 2009, **33**: 18
23 Gyulassy M, Frankel K, Relmer E A. Nucl. Phys. A, 1983, **402**: 596
24 Mattiello R et al. Phys. Rev. C, 1997, **55**: 1443; Oh Y, Ko C M. Phys. Rev. C, 2007, **76**: 054910
25 Polleri A et al. Nucl. Phys. A, 1999, **661**: 452
26 Aerts A T M, Dover C B. Phys. Rev. D, 1983, **28**: 450; Chen L W, Ko C M. Phys. Rev. C, 2006, **73**: 044903
27 Li B A, Ko C M. Phys. Rev. C, 1995, **52**: 2037
28 Bertsch G F, Gupta S Das. Phys. Rep., 1988, **160**: 189; Li B A, Bauer W. Phys. Lett. B, 1991, **254**: 335
29 Baldini A, Flaminio V, Moorhead W G, Morrison D R O. Total Cross-sections for the Reactions of high Energy particles. Berlin: Springer-Verlag, 1988. 102
30 Merschmeyer M et al. Phys. Rev. C, 2007, **76**: 024906
31 Justice M et al. Phys. Lett. B, 1998, **440**: 12
32 Shen W Q et al. Nucl. Phys. A, 1989, **491**: 130
33 Xu Z B. J. Phys. G: Nucl. Part. Phys., 1999, **25**: 403
34 Barrette J et al. Phys. Rev. C, 1994, **50**: 1077